Lab on a Chip

RSC Publishing

PAPER

View Article Online
View Journal | View Issue

Microfluidic heart on a chip for higher throughput pharmacological studies†

Cite this: *Lab Chip*, 2013, **13**, 3599

Ashutosh Agarwal, Josue Adrian Goss, Alexander Cho, Megan Laura McCain and Kevin Kit Parker*

We present the design of a higher throughput ''heart on a chip'' which utilizes a semi-automated fabrication technique to process sub millimeter sized thin film cantilevers of soft elastomers. Anisotropic cardiac microtissues which recapitulate the laminar architecture of the heart ventricle are engineered on these cantilevers. Deflection of these cantilevers, termed Muscular Thin Films (MTFs), during muscle contraction allows calculation of diastolic and systolic stresses generated by the engineered tissues. We also present the design of a reusable one channel fluidic microdevice completely built out of autoclavable materials which incorporates various features required for an optical cardiac contractility assay: metallic base which fits on a heating element for temperature control, transparent top for recording cantilever deformation and embedded electrodes for electrical field stimulation of the tissue. We employ the microdevice to test the positive inotropic effect of isoproterenol on cardiac contractility at dosages ranging from 1 nM to 100 μM. The higher throughput fluidic heart on a chip has applications in testing of cardiac tissues built from rare or expensive cell sources and for integration with other organ mimics. These advances will help alleviate translational barriers for commercial adoption of these technologies by improving the throughput and reproducibility of readout, standardization of the platform and scalability of manufacture.

Received 18th March 2013,
Accepted 17th June 2013

DOI: 10.1039/c3lc50350j

www.rsc.org/loc

Introduction

Preclinical drug development is severely hampered by high failure rates due to cardiac side effects.[1] In addition, unforeseen cardiac toxicities are also a growing concern not only for clinical trials but also for already marketed drugs.[2] Hence, the importance of developing relevant *in vitro* platforms which recapitulate cardiac tissue level functionality to cheaply and reliably test drug candidates has recently been recognised. It is envisioned that these platforms would eventually be human relevant and hence, provide a solution to the challenges of inter-species differences and high costs involved with whole animal testing.[3–7] There is a clear and unmet need to develop tools which will aid the development of such platforms.[8] The development of such tools will be dictated by the goals of faithful recapitulation of cardiac physiology and function as well as amenability to extract high information data in a high throughput fashion.

It has been shown that both single cell studies as well as studies on isotropic layers of cardiac myocytes are not an appropriate model for all types of toxicology studies.[9] Hence, techniques have been developed to engineer anisotropic cardiac cells and tissues on top on elastomeric substrates.[10–12] The Muscular Thin Film (MTF)[13] assay measures contractile stresses generated by 2D bilaminate constructs consisting of anisotropic muscular tissue engineered on top of a deformable elastic thin film.[14] The contractility of the engineered tissue is derived from the observation of the three-dimensional (3D) deformations of MTFs. The assay has been employed for evaluating contractility and tissue structure from multiple tissues in the same experiment.[15–17] Other competing tissue level cardiotoxicity screening technologies either do not recapitulate the *in vivo* tissue architecture[18–21] or are not amenable to a higher throughput translation.[22]

In this report, we advance the throughput of MTF technology based heart on a chip by an order of magnitude through computer aided design and laser based fabrication of thin PDMS cantilevers. Our laser fabricated platform has a throughput comparable to those of commercially available impedance based cardiotoxicity assays[23–26] while still inheriting the advantages of already established MTF technology: (i) Engineered tissues which better recapitulate *in vivo* physiology and (ii) quantification of multiple relevant bioanalytics such as tissue structure, contractility, and electrophysiological properties. Furthermore, we incorporate the chip in a novel microdevice which enables fluidic control over drug wash-in

Disease Biophysics Group, Wyss Institute of Biologically Inspired Engineering, Harvard Stem Cell Institute, School of Engineering and Applied Sciences, Harvard University, 29 Oxford St, Pierce Hall Rm 321, Cambridge, MA, 02138, USA. E-mail: kkparker@seas.harvard.edu; Fax: +1 617 495 9837; Tel: +1 617 495 2850

† Electronic supplementary information (ESI) available. See DOI: 10.1039/c3lc50350j

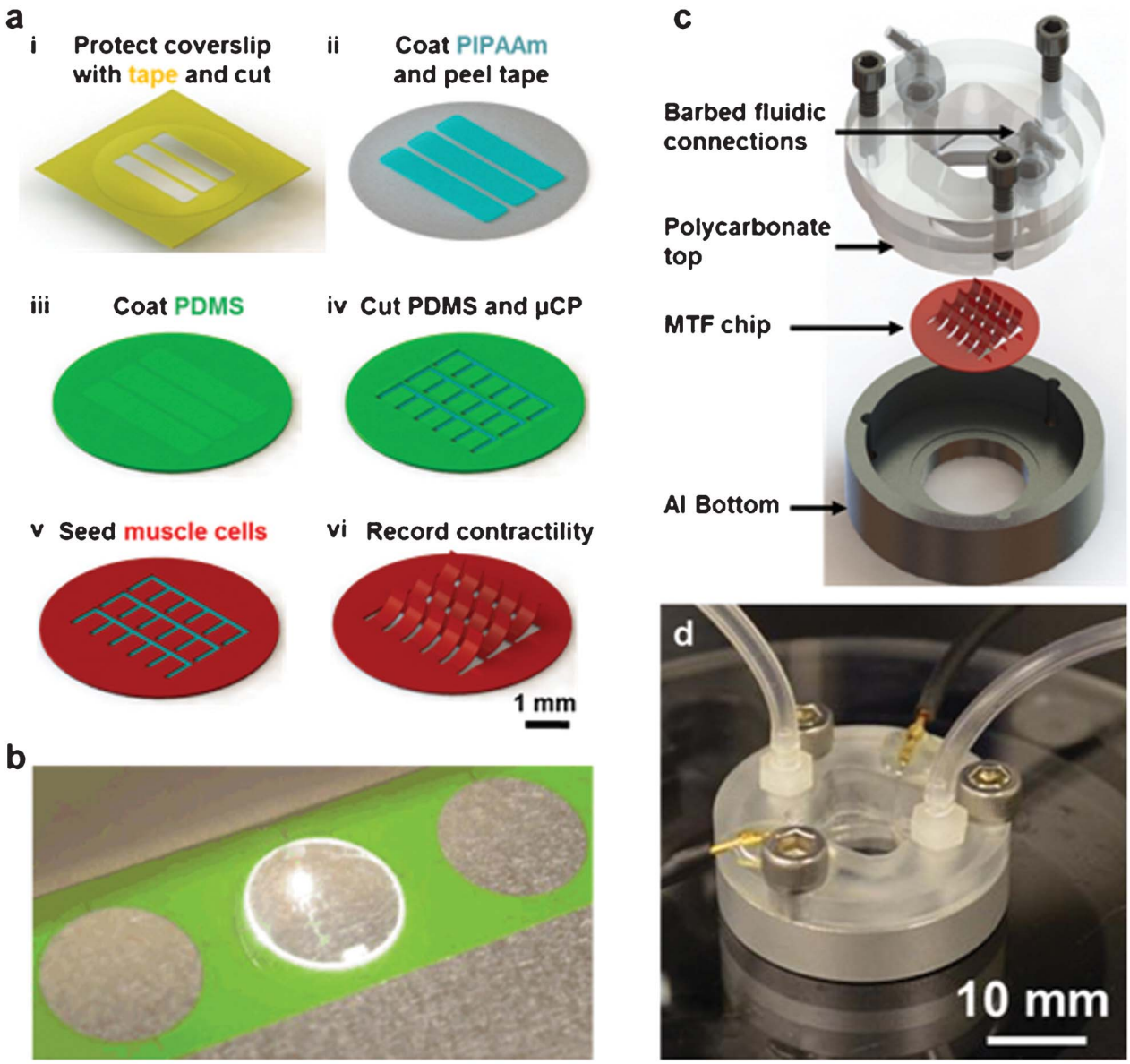

Fig. 1 Higher throughput heart on a chip and fluidic microdevice. (a) A schematic of fabrication process (i) A glass coverslip is covered with protective tape and PIPAAm islands are cut into by an engraving laser and peeled using a sharp tweezer. (ii) A thin layer of PIPAAm is spun coat, (iii) the tape is removed and PDMS is spun coat. (iv) The boundaries of thin films are then cut into the PDMS and peeled. (v) The chip is then ready for micro contact printing of fibronectin and cell seeding. (vi) Upon PIPAAm dissolution, individual MTFs are released from the surface and interrogated optically. (b) Image of the engraving laser processing MTFs in an 18 mm diameter chip. A batch of multiple chips can be fabricated by this computer aided design process. (c) Exploded view of the conception and assembly of a fluidic device which fits an 18 mm chip. The device consists of an aluminum bottom with a recess to hold the chip, a transparent polycarbonate top held in place by three screws and barbed fittings for fluidic input and output. (d) Image of an actual device in action. The connection for electrical field stimulator can also be seen in addition to the fluidic tubing.

wash-out experiments. The microdevice has a heated metallic base for maintaining physiological temperatures, transparent top for optically recording MTF deformation and embedded electrodes for electrical field stimulation of the tissue. We believe that the advances reported here will help alleviate several translational barriers in commercial adoption of this platform.

Results

Laser based chip fabrication

We sought to semi-automate the fabrication and operation of our MTF based heart on a chip platform. In order to complete all of the chip fabrication steps before cell seeding and culture, we employed a commercially available laser engraver to manufacture the chips. As illustrated in Fig. 1a (i), we first

masked the surface of clean glass coverslips with low-adhesion tape. In order to create surface patterns of poly(*N*-isopropylacrylamide) (PIPAAm), rectangular islands were cut into the tape and peeled. The cuts left a shallow engraving mark into the glass which helped in optically registering the MTF cuts into the PDMS layer with respect to the location of PIPAAm islands (Fig. 1a (ii–iii)). Upon cutting the outline of sub millimeter sized MTFs into the PDMS layer (Fig. 1a (iv)), the chips were ready for microcontact printing, cell seeding, culture, and contractility assay (Fig. 1a (v–vi)). Closely spaced lines of fibronectin were microcontact printed on the PDMS layer along the length of the cantilevers to induce the self-assembly of cardiac myocytes into 2-D laminar anisotropic tissues, mimicking the native tissue architecture of the ventricle.

The entire chip fabrication process was designed in Corel Draw, a vector based drawing software which facilitates sequential cuts on several chips without chip realignment. As shown in Fig. 1b, multiple chips were laid down (with the location of each chip recorded in the laser CAD software) and the laser engraver processed them in a batch fashion. Hence, a semi-automated laser cutting of cantilevers was successfully developed which conferred us the ability to fabricate much smaller films of standard and reproducible dimensions in a batch process.

Design of the fluidic microdevice

We asked if MTF readout, which is typically carried out in an open well configuration, could be conducted in a fully enclosed fluidic microdevice. This is highly desirable for developing scaled and interconnected multi organ systems which support fluidic control elements such as barbed fittings, small bore tubing, microfabricated pumps, and valves. Our design was also constrained by the choice of materials which typically do not absorb or adsorb small molecule drugs and are autoclavable.

To accommodate the MTF chip, we designed an aluminum well shaped chamber with a 15 mm diameter hole in the bottom which would allow optical readout of contractility (device geometry and dimensions detailed in Supplementary Fig. 1a, ESI†). A 0.5 mm deep recess was micromachined on the bottom surface to hold the 18 mm diameter MTF chip. The overall diameter, height, and thickness of the aluminum chamber was 35 mm, 7.5 mm, and 2.5 mm, respectively. For creating a fluidic top, we designed a complementary piece built out of polycarbonate which had additional barbed fluidic connections (details in Supplementary Fig. 1b, ESI†). Fluidic channels from both ends fed into a fluidic chamber micromachined into the polycarbonate. Due to the symmetric nature of the design, the ceiling of the fluidic chamber was situated right above the MTF chip and allowed a clearance of 5 mm for the contraction of approximately 1 mm long MTFs away from the glass coverslip. Three fastener holes were milled into the polycarbonate and aluminum pieces to hold tightening screws. Additionally, we manually punched out small holes into the polycarbonate top to thread in 0.5 mm diameter platinum wires and seal off the holes with medical grade epoxy. An exploded drawing view of the device illustrating the various components of microdevice assembly is shown in Fig. 1c and a photograph of an assembled microdevice is shown in Fig. 1d. Thus, we designed and fabricated a novel one channel fluidic microdevice built from reusable and autoclavable materials which incorporates various features required for an optical cardiac contractility assay: metallic base which fits on a heating element for temperature control, transparent top for recording cantilever deformation, and embedded electrodes for electrical field stimulation of the tissue.

Operation of the higher throughput fluidic microdevice

We tested the fluidic microdevice for collection of accurate contractile functional and quantitative structural data. MTF chips were fabricated according to the above described protocol and contractility experiments were carried out 4 days post seeding of cardiac myocytes. For operation of the microdevice, an MTF chip was brought from the incubator and placed in the aluminum chamber. The polycarbonate top was tightly fastened creating a fluidic seal between the top and PDMS coated MTF chip. Barbed inlet fitting was connected to a 10 ml syringe mounted on a syringe pump through Sani-Pure™ 60 tubing. The entire system volume (including the microdevice, barbed fittings and tubing) was approximately 3 ml. Infusions of 10 ml at a flow rate of 1 ml min^{-1} were employed for complete flush out of the system. The ends of the platinum wire were connected to an external field stimulator and microtissues were electrically stimulated at 2 Hz with 10–15 V of a bipolar square pulse of 10 ms duration to stimulate membrane depolarization.

Images of the chip during diastole (Fig. 2a) and peak systole (Fig. 2b) reveal that each MTF contracts freely under external field stimulation and is amenable for contractility determination. The action of a few MTFs (depicted by red and green squares) during diastole and peak systole is shown in Fig. 2c and 2d, respectively. Fig. 2e depicts the contractility endpoints collected from this chip collected over four contraction cycles. We were able to quantify diastolic stress (plotted in red), peak systolic stress (plotted in green), and the twitch stress (plotted in gray) from almost each MTF on the chip. The stress values for each MTF represent Mean $\pm$ SD for four contraction cycles. For this particular chip, we calculated an average peak systolic and twitch stress of 15.4 $\pm$ 1.4 kPa and 12.7 $\pm$ 1.1 kPa, respectively, (Mean $\pm$ SEM, N = 35 MTFs) which matches very well with values reported from MTF experiments conducted in open well configuration[14,16,17,27] and from contractility measurement of isolated rat papillary muscle.[28]

Furthermore, upon the completion of contractility experiments, we immunostained the MTF chip for nuclei, actin, and sarcomeric α-actinin to directly compare the stress generated by each tissue on the chip relative to its sarcomere organization. Immunostains for the MTF highlighted by the yellow box in Fig. 2c are shown in Fig. 2f (actin and nuclei) and 2g (sarcomeric α-actinin). Thus, our higher throughput microdevice retains the advantages of the MTF platform and is amenable to structural and functional endpoint measurements.

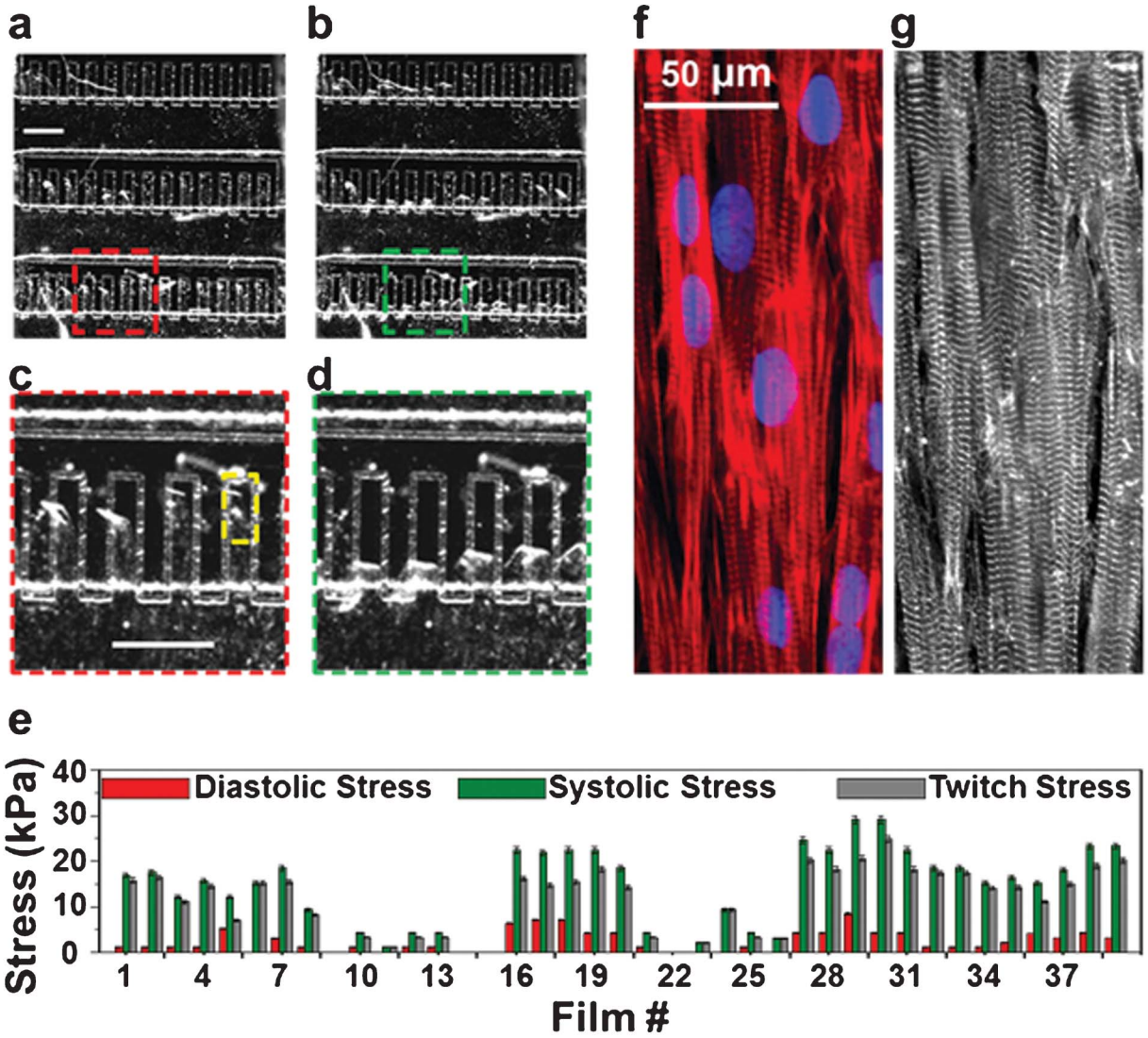

Fig. 2 Operation of the higher throughput heart on a chip. Brightfield image of the chip during (a) diastole and (b) peak systole. Scale bar in (a) represents 1 mm. Films bend up during diastole and their contraction is more pronounced during peak systole. Note that the abrasion into glass indicate the location of PIPAAm island and the boundary of each MTF before contraction. (c) and (d) represent the zoomed sections of (a) and (b), respectively as indicated for better clarity. Scale bar in (c) represents 1 mm. (e) Diastolic, peak systolic and twitch stresses for each MTF from this chip are plotted (Average ± SD for four contraction cycles). In this representative example, operation of one higher-throughput chip provided 35 replicates and an average twitch stress of 12.7 ± 1.1 kPa (N = 35, Mean ± SEM). Immunostain overlay of the (f) actin filaments (red) and nuclei (blue) and (g) α-actinin show the formation of anisotropic confluent monolayer formation of cardiac tissue on thin film area indicated by yellow rectangle in (c).

Evaluation of structure–function relationship

We asked if our platform could be employed for quick execution of studies which aim to link changes in tissue architecture to resultant changes in contractile output. For this purpose, we designed photolithographic masks which yielded 15 μm lines of fibronectin separated by 2, 3, 4, and 5 μm. MTF chips were prepared with each of these patterns, and subsequent to contractility measurements, were fixed and immunostained for fibronectin (Fig. 3a), nuclei (Fig. 3b), actin (Fig. 3c), and α-actinin (Fig. 3d). Operation of just one MTF chip per condition yielded at least 28 MTFs for contractility endpoints for each condition and they are plotted in Fig. 3e. The variability between MTFs from the same chip can be attributed to the stochasticity in the number of cells that land on each MTF and localized variation in the quality of micropatterning leading to differences in the contractile strength of engineered tissue on each MTF. Data collection from these four chips took approximately 4 man-hours and we employed 1.6 million cells in the process. Even though we were not able to detect statistical differences in diastolic, peak systolic or twitch stresses between the four conditions, this example demonstrates the utility of our method in obtaining a high number of replicates with just one experiment.

Next, we sought to compare the anisotropy in intracellular architecture between the cultures on these four different

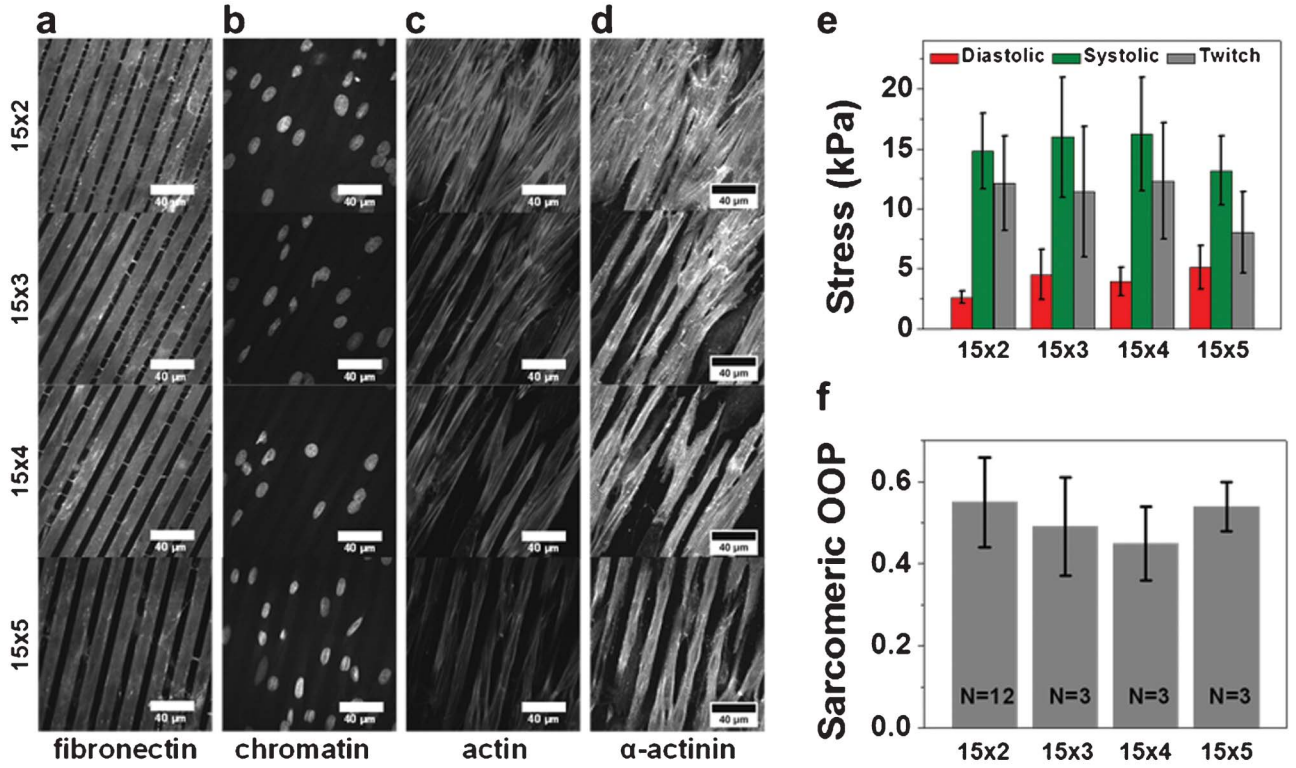

Fig. 3 Application of the higher throughput chip towards evaluation of the effect of tissue architecture on tissue contractility. Immunostains of tissue prepared by micropatterning 15 μm lines of fibronectin separated by gaps of 2 (Panel i), 3 (Panel ii), 4 (Panel iii) and 5 μm (Panel iv). Panel a, b, c, d show the fluorescence images of immunostains for fibronectin, chromatin (DAPI), actin, and sarcomeric α-actinin, respectively. Fibronectin immunostain reveal that microcontact printed fibronectin matched accurately the feature geometry of the stamp. (e) Peak diastolic, systolic and twitch stresses calculated from one chip for each condition (Mean ± SEM, N = 30 for 15 × 2, N = 28 for 15 × 3, N = 30 for 15 × 4, N = 34 for 15 × 5). (f) Orientational order parameter (OOP) for sarcomeric alignment in cardiac tissue engineered with different surface patterns. (Mean ± SD, N indicated on the bar graphs represent the number of chips for each condition with at least 3 fields of view of 160 μm × 160 μm per chip).

patterns. Quantification of sarcomeric alignment was carried out using a modified fingerprint detection algorithm[13] previously developed to quantify sarcomeric Orientational Order Parameter (OOP).[16] OOP is extensively used in the analysis of spatial order in liquid crystals and ranges from a value of zero for completely random and isotropic sample to unity for perfectly aligned sample.[29] Indeed, even though sarcomeric OOP (plotted in Fig. 3f) matched very well the values reported for anisotropic tissues;[14,16,27] it did not reveal any statistical differences for tissues engineered on the four patterns. Nevertheless, through this test case, we were able to demonstrate that a high throughput evaluation of structure-function relationship is feasible with our platform.

Isoproterenol dose response studies

We sought to test the fluidic microdevice for evaluating the *in vitro* response of engineered cardiac microtissues to pharmacological agents. Beta-adrenergic receptors in the cardiac system have been extensively studied and targeted for positive and negative inotropic compound discovery and preventing drug cardiotoxicity.[30–32] Isoproterenol is a non selective beta-adrenergic agonist and has been well characterized for its treatment of bradycardia. We decided to test the *in vitro* effect of isoproterenol on electrically stimulated cardiac microtissues within our microdevice. Control experiments were carried out in drug-free condition and the system was exposed to tenfold sequential increases in the dosage of drug by flushing in the solution of the drug dissolved in Tyrode's. Changes in contractile output of MTFs were calculated over four contraction cycles at each drug dosage. Fig. 4a depicts the image the device in operation and Fig. 4b plots the percentage changes in twitch stress from baseline (established in the control condition) in response to increasing drug concentration. We were able to create 19 replicates from the same fluidic chip and generate a pD2 value of 5.75 from our drug dose response data. Both the responses and pD2 value are similar to the responses reported in literature for rat heart[33,34] and from *in vitro* experiments.[35] Fig. 4c and 4d plot the contractile endpoints from the same chip in the control experiment (no drug exposure) and at 10^{-4} M exposure to isoproterenol, respectively. For each MTF shown (and numbered) in Fig. 4a, the lower Y intercept of the bar graphs in Fig. 4c and 4d depict the diastolic stress, the upper Y intercept depicts the peak systolic stress, the length of the bar depicts the twitch stress and the error bars for diastolic and peak systolic stress depict the standard deviation over four contraction cycles. The results

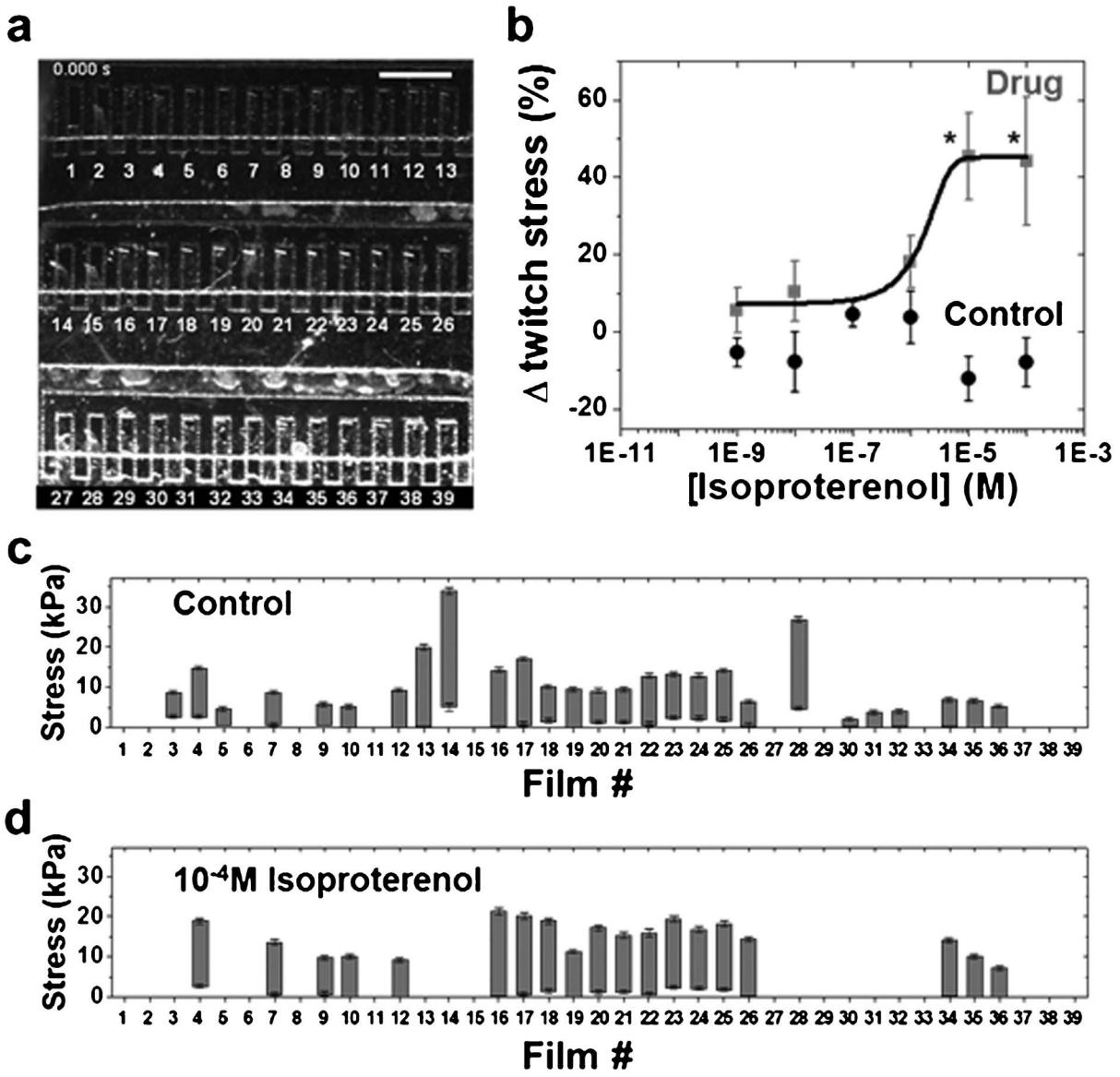

Fig. 4 Evaluation of the effect of isoproterenol on cardiac contractility. (a) Brightfield image of a higher throughput chip during drug dose response studies within the fluidic microdevice. Scale bar represents 1 mm. (b) Complete isoproterenol dose response curve (data points represented by gray squares) generated from the operation of one fluidic chip (N = 19 MTFs, Mean ± SEM, * = statistically different from baseline, $p < 0.05$). Black circles represent the data points for control experiment to evaluate cardiac contractility in the absence of isoproterenol. Drug-free Tyrode's solution is injected into the fluidic device at the same time points as for conducting drug dose response studies (N = 23 MTFs, Mean ± SEM). (c) Baseline stresses (before exposure to isoproterenol) of individual MTFs. Minima, maxima and the length of the each bar graph represent the diastolic, peak systolic, and twitch stress generated by the corresponding MTF, respectively. Error bars for diastolic and peak systolic stress represent the standard deviation in the average measurement over four contraction cycles. (d) Stress generated by the same MTFs at the highest isoproterenol concentration of 10^{-4} M.

from a control experiment, where drug-free Tyrode's solution was infused at the same time points, are also plotted in Fig. 4b (black circles). The control experiment shows that MTFs maintain their baseline strength of contraction over a long period of time in the absence of drug. Hence, the fluidic microdevice encompassing a higher throughput laser MTF chip provides a simple and robust measurement of contractility changes in response to drug dose exposure.

Discussion

There is a rapidly growing interest in developing human relevant organ on chip platforms to measure efficacy and toxicity of drugs, and the effects of pollutants and pathogens. Ideally, these organ mimics need to be microfluidically linked with each other to enable studies of inter organ interactions. This is a grand challenge as every organ mimic has its own set of design constraints. MTF based platforms recapitulate the *in*

vivo physiology of muscle architecture and provide quantifiable structure and contractile functional endpoints. However, MTFs require considerable free volume to contract freely away from the substrate. This precludes direct implementation of highly complex microfluidic devices[36] which promise high throughput.[37] Hence, we focused on designing a simple one channel fluidic device which is reusable (almost all the components of the device are autoclavable), does not require specialized skills for operation (screws for reversible sealing of the device and optical readout of contractility), and addressees issues such as biocompatibility of materials (SaniPure™ 60 tubing is entirely non-cytotoxic and non-absorbing and has a smooth inner bore which reduces microscopic build up), maintenance of sterility and formation of air bubbles. Apart from the very thin layer of PDMS, none of the materials that come in contact with the drug infused buffer are absorbing materials.

We also focused on minimizing user handling of the chip and increasing the throughput of readout. To protect the engineered tissue from environmental exposure before data collection, all the chip fabrication steps are completed before cell culture. We are able to produce up to 50 replicates from a chip with a cell requirement of 0.4 million cardiac myocytes cells, hence significantly advancing the throughput of our MTF technology. All the MTFs are of standard and reproducible dimensions, hence improving the reproducibility of readout. The dual laser cuts were processed routinely in a batch of up to 25 chips, which portends well for the scalability of manufacture.

Several components to testing our fluidic organ on chip device included the correlative case study for linking tissue architecture and contractility and changes in tissue function during pharmacological challenge. In the first case study, one could qualitatively discern a near monolayer coverage with 15 μm × 2 μm pattern and incomplete separation between lines of tissues with gaps of 3, 4, and 5 μm. A stronger contractile output has been reported with engineered lines of cardiac tissue as opposed to anisotropic monolayers.[27] Indeed, all of our engineered tissue conditions seem to fall somewhere in between a monolayer coverage and well separated lines. Nevertheless, it does not diminish the fact that an experiment with just one chip can provide ample replicates to inform a decision about optimal surface pattern. This is critically important when working with a new cell source which is rare and/or expensive (such as human iPS derived cardiomyocytes and primary human cardiomyocytes). Isoproterenol dose response studies reveal the potential utility of the platform in simultaneously measuring the contractile function of multiple tissues during pharmacological interventions. Tissues were acutely exposed to different drug concentrations with complete washout between dosages leading a fast collection of high quality functional data from just one chip. It should be noted that complete flushing between incremental dosages is technically difficult to perform in an open well configuration with freely beating MTFs.

The advances reported here with the fluidic microdevice design, fabrication and operation can be directly implemented in creating fluidic organ mimics of vascular and bronchial smooth muscle tissue. Since the form factor of the fluidic device design of striated and smooth muscle mimics would remain basically the same, the fluidic integration should be straightforward and will pave the way for coupled organ on chip initiatives. The fluidic microdevice is amenable to both rapid and continuous perfusion of drug solutions and hence, *in vitro* drug testing studies for different exposure regimes are feasible. Furthermore, these microdevices could be applied towards creating diseased organ mimics by continuous perfusion of signaling molecules such as small cytokines which could lead to the first demonstration of coupled diseased organ mimics.

Experimental

Chip fabrication

18 mm diameter circular glass coverslips (Product# 26022, Ted Pella Inc. Redding CA) were used as substrates for chip fabrication. Coverslips were cleaned by sonication in 95% ethanol solution for 60 min. Clean coverslips were immediately covered with low adhesion Scotch-Blue™ painter's tape (Product# 2080, 3M, St. Paul, MN). Four rectangular shapes with rounded edges of dimensions 10 mm × 2 mm were cut into the tape with a CO_2 laser prototyping system (VersaLaser 2.0, 10.6 micron wavelength, 50 W, Universal Laser systems, Scottsdale, AZ) using 1% Power and 10% Speed settings. These rectangular shapes were removed from the coverslip using a sharp tweezer. A 10% (w/v) solution of poly(*N*-isopropylacrylamide), PIPAAm, (Polysciences, Inc., Warrington, PA) in 99% butanol was spun coat on these partially tape-covered coverslips at a top speed 6000 rpm for 1 min using a spin coater placed in a chemical hood (G3P8 Speciality Spin Coater, SCS Inc., Indianapolis, Indiana). The rest of the tape was carefully peeled from the coverslips and Polydimethylsiloxane, PDMS (Sylgard 184 elastomer, Dow Corning, Midland, MI) mixed at 10 : 1 base to curing agent ratio was spun coat on the partially PIPAAm covered coverslip at a top speed of 4000 rpm for 1 min. PDMS coated chips were placed in a 65 °C for at least 8 h to allow complete curing of the elastomer. In the final step, 1 row of cantilever outlines was laser cut into the PDMS layer within each PIPAAm rectangular regions with 0.2% Power and 0.1% Speed settings such that the final cantilevers were 1.2 mm × 0.3 mm and spaced 0.6 mm apart (vertical center to center distance). The second laser cut (into Sylgard 184) was aligned with the first cut such that the bottom edge of the cantilevers would be situated approximately 0.2 mm beyond the PIPAAm rectangle edge. Cuts were designed using CorelDRAW graphic design software (Corel Inc., Ottawa, Canada) and up to 20 chips were batch processed for cuts into Scotch tape and PDMS. For each batch of chips, thickness of the PDMS elastomer layer was measured using a contact profilometer (Dektak 6M, Veeco Instruments Inc., Plainview, NY).

For anisotropic cardiac myocyte tissue generation on MTFs, 15 μm lines of human fibronectin (BD Biosciences, Sparks, MD) separated by 2 to 5 μm spacing was microcontact printed along the long axis of MTFs. Briefly, PDMS stamps were incubated with fibronectin (50 μg mL^{-1} in water) for 45 min, air dried and brought briefly into contact with MTF chips which had been exposed to UV ozone for 8 min (Model# 342, Jetlight Company Inc., Phoenix, AZ). Stamped coverslips were stored dry at 4 °C.

Fluidic microdevice design and fabrication

The fluidic microdevice was designed using a 3D CAD software (SolidWorks, Dassault Systèmes Corp., Waltham, MA) and subsequently custom CNC micro-machined (Proto Labs Inc., Maple Plain, MN). The aluminum bottom dish had an external diameter of 35 mm, overall height of 7.5 mm, with a cylindrical cavity of height 5 mm and diameter 30 mm cut into it, leaving behind a bottom layer and side walls of thickness 2.5 mm each. The bottom layer had a 0.5 mm deep recess of diameter 18 mm to hold the chip and a through hole of diameter 15 mm to optically image the chip. Three symmetrically placed threaded holes with diameter 2.3 mm were milled into the wall of the device for fitting the fluidic top. The top piece was machined out of polycarbonate and had two barbed fittings with single channels feeding into an 11.5 mm × 11.5 mm fluidic chamber which was 2.5 mm deep. A square hole (edge 11.43 mm, depth 9.525 mm, and R3.175 corners) is first through cut in the middle of flow cell chamber lid and a second square pocket (edge 15.24 mm, depth 7.525 mm, and R3.175 corners, rotated 45 degrees from the through cut) was then machined in order to create an optically-clear observation pocket. A micromachined 15 mm square piece of polycarbonate was solvent bonded into the pocket. Liquid acetone was applied to the contacting surfaces using cotton tipped applicators and the parts were brought into contact and clamped overnight at room temperature. Similar to the aluminum bottom, three symmetrically placed threaded holes were milled into it. Field stimulation electrodes built from 0.5 mm diameter platinum wire (VWR, Radnor, PA) were manually threaded into the polycarbonate top through holes created with sharp punches and sealed using medical grade urethane adhesive (Loctite® M-11FL™, R.S. Hughes Inc., Sunnyvale, CA).

Cardiac myocyte harvest, seeding and culture

All procedures were conducted according to the guidelines of the Harvard University Animal Care and Use Committee. Cardiac myocytes were extracted from the ventricles of two day old neonatal Sprague-Dawley rats (Charles River Laboratories, Wilmington, MA) using previously described protocols.[38] Briefly, cardiac myocytes were isolated from ventricles that were extracted and washed in Hanks balanced salt solution; they were then digested with trypsin overnight at 4 °C and collagenase at 37 °C for several minutes, followed by mechanical agitation by pipetting. Isolated cells were re-suspended in M199 culture medium supplemented with 10% heat-inactivated fetal bovine serum (FBS, Invitrogen, Carlsbad, CA), 10 mM HEPES, 0.1 mM MEM non-essential amino acids, 20 mM glucose, 2 mM L-glutamine, 1.5 μM vitamin B-12, and 50 U mL^{-1} penicillin. MTF chips were seeded in 12-well plates at a density of 100 000 cells cm^{-2}. After 1 day, samples were washed twice with PBS and reincubated in fresh culture medium with 10% FBS. On day 2, the serum concentration was reduced to 2% in order to reduce fibroblast proliferation. Cells were cultured for 4 days prior to conducting the experiments.

Contractility assay

Contractility assay was performed outside the incubator on a stereomicroscope (Model MZ6, Leica Microsystems Inc., Wetzlar, Germany) coupled to a National Instruments LabVIEW data acquisition board. All experiments were performed in warm Tyrode's solution (1.192 g l^{-1} HEPES, 0.040 g l^{-1} NaH_2PO_4, 0.901 g l^{-1} glucose, 0.265 g l^{-1} $CaCl_2$, 0.203 g l^{-1} $MgCl_2$, 0.403 g l^{-1} KCl, 7.889 g l^{-1} NaCl, pH adjusted to 7.4 using 1N NaOH, all chemicals from Sigma-Aldrich, St. Louis, MO). The temperature of Tyrode's solution was briefly allowed to go below 32 °C to effect the phase transition of PIPAAm. MTFs were gently peeled up using sharp tweezers and the chip was placed onto the bottom aluminum piece of the microdevice and secured tightly with the polycarbonate top with three screws to create a fluidic seal between the PDMS coated chip and polycarbonate top. The device was filled with warm Tyrode's using a 10 ml syringe, electrodes were connected to an external field stimulator (Myopacer, IonOptix Corp., Milton, MA), and the microdevice was placed on a heating plate so that experiments could be performed at 37 °C. Electrical field stimulation was performed at 2 Hz and the chip was filmed throughout the experiment at a frame rate of 100 fps. The stimulation voltage was set at 20% above the voltage at which approximately 90% of the MTFs would be captured with the specified frequency.

Isoproterenol dose experiment

Isoproterenol hydrochloride (Sigma-Aldrich) was serially dissolved in freshly prepared Tyrode's solution. The fluidic microdevice was coupled to remote infusion syringe pump (PHD Ultra, Harvard Apparatus, Holliston, MA) through its barbed fittings and autoclavable Sani-Pure™ 60 tubing (Saint-Gobain Performance Plastics, Akron, OH). 10 ml syringes in the infusion pump were filled with either pure Tyrode's or Tyrode's containing drug and a flow rate of 1 ml min^{-1} was employed. The system volume was approximately 3 ml and hence an injection of 10 ml ensured a complete flush with new solution. Control experiments were carried out in drug-free condition and the system was subsequently exposed to 1.0 logarithmic increases in the concentration of drug.

Contractility analysis

The *x*-projections of contracting MTFs were detected using custom ImageJ (NIH, Bethesda, MD) software and used to derive the radius of curvature using previously reported custom MATLAB (Mathworks, Natick, MA) code.[16] Radius of curvature, stiffness, and thickness of the hybrid construct was used to calculate the stress generated using a previously published model.[14] MTFs which were either damaged during the handling of the chip, or did not pace with the electrical field stimulation were excluded from contractility analysis. No

other exclusion criterion (for example, statistical outliers *etc.*) was imposed.

Immunostaining, imaging and analysis

Subsequent to contractility experiments, MTF chips were incubated in a warm solution of 4% Paraformaldehyde (PFA) and 0.5 μl ml^{-1} of TritonX-100 in PBS. After 15 min, samples were washed with PBS and placed upside down on 200 μl of a solution of PBS containing 1 μl DAPI, 1 μl Alexa Fluor633-conjugated Phalloidin (A22284, Invitrogen, Carlsbad, CA), 1 μl polyclonal anti-human fibronectin antibody (F3648, Sigma-Aldrich), and 1 μl monoclonal anti-sarcomeric α-actinin (A7732 clone EA-53, Sigma-Aldrich) for 1 h at room temperature. Samples were then triple rinsed in PBS and incubated for 1 h with the corresponding goat anti-mouse Alexa Fluor-488 (A-11001, Invitrogen) secondary antibody for α-actinin and goat anti-rabbit Alexa Fluor-546 (A-11035, Invitrogen, Carlsbad, CA) secondary antibody for fibronectin. The samples were then triple rinsed in PBS and mounted on microscope glass slides before fluorescent imaging on a Zeiss LSM 7 LIVE confocal microscope. Fluorescent immunostains of α-actinin were processed using a MATLAB code based on fingerprint detection as previously reported. After extraction of the main pattern, the angle distribution was analyzed and orientational order parameter (OOP) reported. The OOP and stress data were compared with a one-way analysis of variance (ANOVA) with a pair wise comparison significance computed with a Tukey test.

Conclusions

Here, we report two advances towards building a fluidic heart on a chip: (i) Laser based fabrication of sub millimeter sized cantilevers of standard and reproducible dimensions in a batch process amenable to an assembly line type of fabrication and (ii) a novel fluidic microdevice which incorporates various features required for an optical cardiac contractility assay. The fluidic microdevice is employed towards collecting accurate functional contractile responses to a cardiac drug and exploring structure function relationships. The technology is ideally suited for generating large amounts of high quality functional data, *in vitro* drug testing studies, incorporation of tissues engineered from costly cell sources and fluidic linkage with other organ mimics.

Acknowledgements

We acknowledge the support from Harvard Materials Research Science and Engineering Center under NSF award number DMR-0213805, NIH/NINDS grant 1 U01 NS073474-01, and the Harvard Center for Nanoscale Systems for the use of clean room facilities.

References

1 E. L. Eisenstein, P. W. Lemons, B. E. Tardiff, K. A. Schulman, M. K. Jolly and R. M. Califf, *Am. Heart J.*, 2005, **149**, 482–488.
2 B. Fermini and A. A. Fossa, *Nat. Rev. Drug Discovery*, 2003, **2**, 439–447.
3 D. Huh, Y. S. Torisawa, G. A. Hamilton, H. J. Kim and D. E. Ingber, *Lab Chip*, 2012, **12**, 2156–2164.
4 C. Moraes, G. Mehta, S. C. Lesher-Perez and S. Takayama, *Ann. Biomed. Eng.*, 2012, **40**, 1211–1227.
5 A. D. van der Meer and A. van den Berg, *Integr. Biol.*, 2012, **4**, 461–470.
6 A. M. Ghaemmaghami, M. J. Hancock, H. Harrington, H. Kaji and A. Khademhosseini, *Drug Discovery Today*, 2012, **17**, 173–181.
7 D. Huh, G. A. Hamilton and D. E. Ingber, *Trends Cell Biol.*, 2011, **21**, 745–754.
8 M. B. Esch, T. L. King and M. L. Shuler, *Annu. Rev. Biomed. Eng.*, 2011, **13**, 55–72.
9 T. Kaneko, K. Kojima and K. Yasuda, *Analyst*, 2007, **132**, 892–898.
10 P. L. Kuo, H. Lee, M. A. Bray, N. A. Geisse, Y. T. Huang, W. J. Adams, S. P. Sheehy and K. K. Parker, *Am. J. Pathol.*, 2012, **181**, 2030–2037.
11 M. A. P. Bray, W. J. Adams, N. A. Geisse, A. W. Feinberg, S. P. Sheehy and K. K. Parker, *Biomaterials*, 2010, **31**, 5143–5150.
12 N. A. Geisse, S. P. Sheehy and K. K. Parker, *In Vitro Cell. Dev. Biol.: Anim.*, 2009, **45**, 343–350.
13 A. W. Feinberg, A. Feigel, S. S. Shevkoplyas, S. Sheehy, G. M. Whitesides and K. K. Parker, *Science*, 2007, **317**, 1366–1370.
14 P. W. Alford, A. W. Feinberg, S. P. Sheehy and K. K. Parker, *Biomaterials*, 2010, **31**, 3613–3621.
15 P. W. Alford, A. P. Nesmith, J. N. Seywerd, A. Grosberg and K. K. Parker, *Integr. Biol.*, 2011, **3**, 1063–1070.
16 A. Grosberg, P. W. Alford, M. L. McCain and K. K. Parker, *Lab Chip*, 2011, **11**, 4165–4173.
17 A. Grosberg, A. P. Nesmith, J. A. Goss, M. D. Brigham, M. L. McCain and K. K. Parker, *J. Pharmacol. Toxicol. Methods*, 2012, **65**, 126–135.
18 T. Boudou, W. R. Legant, A. B. Mu, M. A. Borochin, N. Thavandiran, M. Radisic, P. W. Zandstra, J. A. Epstein, K. B. Margulies and C. S. Chen, *Tissue Eng. A*, 2012, **18**, 910–919.
19 J. Kim, J. Park, K. Na, S. Yang, J. Baek, E. Yoon, S. Choi, S. Lee, K. Chun, J. Park and S. Park, *J. Biomech.*, 2008, **41**, 2396–2401.
20 J. Park, J. Ryu, S. K. Choi, E. Seo, J. M. Cha, S. Ryu, J. Kim, B. Kim and S. H. Lee, *Anal. Chem.*, 2005, **77**, 6571–6580.
21 P. Linder, J. Trzewik, M. Ruffer, G. M. Artmann, I. Digel, R. Kurz, A. Rothermel, A. Robitzki and A. T. Artmann, *Med. Biol. Eng. Comput.*, 2010, **48**, 59–65.
22 H. Vandenburgh, *Tissue Eng., Part B: Rev.*, 2010, **16**, 55–64.
23 J. D. Cohen, J. E. Babiarz, R. M. Abrams, L. Guo, S. Kameoka, E. Chiao, J. Taunton and K. L. Kolaja, *Toxicol. Appl. Pharmacol.*, 2011, **257**, 74–83.
24 J. Y. Ma, L. Guo, S. J. Fiene, B. D. Anson, J. A. Thomson, T. J. Kamp, K. L. Kolaja, B. J. Swanson and C. T. January, *Am. J. Physiol.: Heart Circ. Physiol.*, 2011, **301**, H2006–H2017.

25 L. Guo, R. M. C. Abrams, J. E. Babiarz, J. D. Cohen, S. Kameoka, M. J. Sanders, E. Chiao and K. L. Kolaja, *Toxicol. Sci.*, 2011, **123**, 281–289.
26 L. Guo, J. Y. Qian, R. Abrams, H. M. Tang, T. Weiser, M. J. Sanders and K. L. Kolaja, *Cell. Physiol. Biochem.*, 2011, **27**, 453–462.
27 A. W. Feinberg, P. W. Alford, H. W. Jin, C. M. Ripplinger, A. A. Werdich, S. P. Sheehy, A. Grosberg and K. K. Parker, *Biomaterials*, 2012, **33**, 5732–5741.
28 S. Nishimura, S. Yasuda, M. Katoh, K. P. Yamada, H. Yamashita, Y. Saeki, K. Sunagawa, R. Nagai, T. Hisada and S. Sugiura, *Am. J. Physiol.: Heart Circ. Physiol.*, 2004, **287**, H196–202.
29 A. Grosberg, P. L. Kuo, C. L. Guo, N. A. Geisse, M. A. Bray, W. J. Adams, S. P. Sheehy and K. K. Parker, *PLoS Comput. Biol.*, 2011, **7**, e1001088.
30 R. Mazza, A. Gattuso, C. Mannarino, B. K. Brar, S. F. Barbieri, B. Tota and S. K. Mahata, *Am. J. Physiol.: Heart Circ. Physiol.*, 2008, **295**, H113–H122.
31 G. Fajardo, M. M. Zhao, G. Barry, D. Mochly-Rosen and D. Bernstein, *Circulation*, 2008, **118**, S485–S486.
32 A. Galindo-Tovar and A. J. Kaumann, *Br. J. Pharmacol.*, 2008, **153**, 710–720.
33 E. N. Juberg, K. P. Minneman and P. W. Abel, *Naunyn-Schmiedebergs Arch. Pharmacol.*, 1985, **330**, 193–202.
34 B. Reza, N. Ali, M. Mustafa, A. Alireza and K. Ali, *Biology and Medicine*, 2009, **1**, 75–81.
35 T. Gulick, S. J. Pieper, M. A. Murphy, L. G. Lange and G. F. Schreiner, *Circulation*, 1991, **84**, 313–321.
36 L. Kim, Y. C. Toh, J. Voldman and H. Yu, *Lab Chip*, 2007, **7**, 681–694.
37 S. T. Yang, X. D. Zhang and Y. Wen, *Current Opinion in Drug Discovery & Development*, 2008, **11**, 111–127.
38 W. J. Adams, T. Pong, N. A. Geisse, S. P. Sheehy, B. Diop-Frimpong and K. K. Parker, *J. Comput.-Aided Mater. Des.*, 2007, **14**, 19–29.

